Received: 5 April 2017 | Accepted: 5 June 2018

DOI: 10.1002/hyp.13214

RESEARCH ARTICLE

WILEY

Transience of seawater intrusion and retreat in response to incremental water-level variations

Antoifi Abdoulhalik[1] | Ashraf A. Ahmed[2]

[1] School of Natural and Built Environment, Queen's University Belfast, Belfast, UK

[2] Department of Civil and Environmental Engineering, Brunel University London, Uxbridge, UK

Correspondence
Antoifi Abdoulhalik, School of Natural and Built Environment, Queen's University Belfast, David Keir Building, Stranmillis Road, Belfast BT95AG, UK.
Email: aabdoulhalik01@qub.ac.uk

Abstract

This paper provides for the first time an experimental study where the impact of sea-level fluctuations and inland boundary head-level variations on freshwater–saltwater interface toe motion and transition zone dynamics was quantitatively analysed under transient conditions. The experiments were conducted in a laboratory flow tank where various (inland and coastal) head changes were imposed to the system and the response of the key seawater intrusion parameters was analysed with high spatial and temporal resolution. Two homogeneous aquifer systems of different grain size were tested. The numerical code SEAWAT was used for the validation. The results show that in cases of sea-level variations, the intruding wedge required up to twice longer time to reach a new steady-state condition than the receding wedge, which thereby extend the theory of timescale asymmetry between saltwater intrusion and retreat processes in scenarios involving sea-level fluctuations. The intruding and receding rates of the saltwater wedge were respectively similar in the scenario involving sea-level and the freshwater-level changes, despite change in transmissivity. The results show that, during the intrusion phase, the transition zone remains relatively insensitive, regardless of where the boundary head change occurs (i.e., freshwater drop or sea-level rise) or its magnitude. By contrast, a substantial widening of the transition zone was observed during the receding phase, with almost similar amplitude in the scenario involving a rise of the freshwater level compared with that caused by a drop of the saltwater level, provided that an equivalent absolute head change magnitude was used. This transition zone widening (occurring during saltwater retreat) was greater and extended over longer period in the low hydraulic conductivity aquifer, for both freshwater-level rise and sea-level drop scenarios. The concentration maps revealed that the widening mechanism was also enhanced by the presence of some freshwater sliding and into the wedge during saltwater retreat, which was thereafter sucked upward towards the interface because of density difference effects.

KEYWORDS

automated image analysis, coastal aquifer, laboratory experiment, numerical modelling, saltwater intrusion, sea-level rise, transient condition, transition zone dynamics

1 | INTRODUCTION

For populations living in coastal zones, which represents about 70% of the world's population (Webb & Howard, 2011), groundwater represents the main, in some cases the only, source of water supply. In such areas, groundwater is particularly susceptible to degradation given its proximity with seawater as well as the intense water demand associated with ever-increasing population densities. The subsequent overabstraction of groundwater to satisfy an increasing demand ultimately leads to the landward incursion of oceanic saline water into fresh coastal groundwater commonly known as seawater intrusion (SWI). Because climate change is expected to aggravate in the near future and thus cause further detrimental effects of SWI, it has become of great importance to further advance the understanding of underlying processes related to SWI for effective water resource management (Werner et al., 2013).

SWI is generally characterized by quantitative indicators, which include external metrics that delineate the outward boundary of the saline plume and the freshwater–saltwater interface. The external SWI metrics include the horizontal extent of intrusion, often called the toe length, and the vertical extent along the coastline boundary (Goswami & Clement, 2007; Sebben, Werner, & Graf, 2015). The freshwater–saltwater interface is a specific characteristic feature of coastal aquifers that occurs as a transition zone (TZ) where the salt concentration varies gradually from that of the freshwater to that of the saltwater in the seaward direction. These parameters outline the wedge-like shape of the plume that the intruding saltwater tend to form while encroaching homogeneous isotropic coastal aquifers, albeit aquifer heterogeneity may, to various degrees, severely affect this highly idealized shape.

In addition to unreasonable extraction of groundwater, climate change also greatly enhances the saltwater intrusion mechanism in coastal aquifers (Ferguson & Gleeson, 2012; Oude Essink, van Baaren, & de Louw, 2010; Sherif & Singh, 1999). The reduction in freshwater recharge, resulting from changes in rainfall patterns, and sea-level rises (SLRs) are the two climate change-induced factors that cause a disruption of the hydraulic gradients between the land and the sea, subsequently leading to more pronounced SWI. The reduction of freshwater recharge into an aquifer induces a direct decrease of the magnitude of the seaward groundwater discharge, which leads to a lesser resistance exerted on the intruding saline water. The rate of freshwater recharge into the aquifer and the magnitude of seaward groundwater discharge are considered the major controlling factors affecting SWI (Ketabchi, Mahmoodzadeh, Ataie-Ashtiani, & Simmons, 2016).

It is often difficult to derive a clear understanding of the mechanisms affecting SWI directly from field-based investigation (Werner et al., 2013). The challenge of measuring and quantifying coastal aquifer hydrodynamics and SWI in field sites has promoted the use of laboratory and numerical modelling tools to gain a valuable insight into SWI response to various geological and/or hydrological stresses, such as (a) change in seaward freshwater discharge resulting from fluctuations at the inland head boundary (Abdoulhalik & Ahmed, 2017a; Abdoulhalik & Ahmed, 2017b; Abdoulhalik, Ahmed, & Hamill, 2017; Goswami & Clement, 2007; Lu & Werner, 2013; Robinson, Ahmed, & Hamill, 2016; Robinson, Hamill, & Ahmed, 2015) in head-controlled systems or from variations of the regional freshwater flux (Chang & Clement, 2012; Stoeckl & Houben, 2012; Stoeckl, Houben, & Dose, 2015) in flux-controlled systems and (b) SLR (Hussain & Javadi, 2016; Morgan, Bakker, & Werner, 2015; Morgan, Stoeckl, Werner, & Post, 2013).

Goswami and Clement (2007) provided a thorough quantitative analysis of the steady state and transient toe response to freshwater head changes to provide an improved benchmark for numerical models. Chang and Clement (2012) examined the difference in the toe response to variations in freshwater flux resulting from regional and areal flow changes. Their study highlighted the difference of timescale associated with saltwater intrusion and retreat and provided explanation of the difference based on flow velocity field analysis. Although these aforementioned studies have emphasized the impact of changes in freshwater flow on saltwater intrusion dynamics, they do not include a quantitative comparison of the toe migration rate in response to inland and coastal head changes. The timescale of toe response was the primary focus of Lu and Werner (2013), whereby the timescale of saltwater intrusion and retreat was related by simple linear empirical correlations to the boundary head difference and distance of toe response, respectively. Although their study examined the timescale of toe response to inland and coastal head changes, their analysis was based on a confined aquifer system, where the saturated thickness remains constant in response to SLR. This study aims to provide a quantitative analysis of the intruding and receding saltwater wedge migration rates in response to inland and coastal head fluctuations in unconfined aquifer systems.

The adverse impact of SLR on SWI has been well documented in the literature (Chang, Clement, Simpson, & Lee, 2011; Ketabchi et al., 2016; Ketabchi, Mahmoodzadeh, Ataie-Ashtiani, Werner, & Simmons, 2014; Michael, Russoniello, & Byron, 2013; Watson, Werner, & Simmons, 2010; Werner & Simmons, 2009). Hussain and Javadi (2016) showed that SLR significantly enhances the inland progression of saline water and caused a substantial reduction of the available fresh groundwater resources, particularly for flat-shoreline aquifer systems. The type of inland boundary condition was found to play a major role in determining the vulnerability of a coastal aquifer to SWI induced by SLR. In physical terms, substantially larger saltwater intrusion lengths have been observed in head-controlled aquifer systems compared with those observed in flux recharge-controlled systems (Michael et al., 2013; Rasmussen, Sonnenborg, Goncear, & Hinsby, 2013; Werner & Simmons, 2009). Several studies gave a special attention to the overshooting mechanism (Ketabchi et al., 2016; Morgan et al., 2013; Morgan et al., 2015; Watson et al., 2010), a process by which the saltwater intrusion length extends transiently beyond the final equilibrium position as a result of SLR, thereby questioning the steady state as being the actual worst case scenario.

Investigations on the impact of sea-level fluctuations on the dynamics (widening and narrowing) of freshwater–saltwater TZ are however very scarce and often limited to numerical modelling works. Lu, Kitanidis, and Luo (2009) explored TZ behaviour under transient flow condition using numerical simulations in a scaled-tank model and field model. They concluded that the widening process was primarily controlled by kinetic mass transfer combined with TZ motion

induced by water-level fluctuations. Lu and Luo (2010) further demonstrated the sensitivity of TZ dynamics to the flow velocity. A comparative analysis of transient TZ dynamics in response to sea-level and freshwater fluctuations from physical experiments, despite their importance in providing insight on underlying processes, is yet to be provided.

This study presents for the first time a quantitative analysis of the response of SWI and retreat to incremental water-level variations under transient condition in physical experiment. The investigation provides transient experimental data set comparing the saltwater wedge toe motion in response to both sea-level and freshwater-level fluctuations, which has never done in previous studies. In addition, the study presents crucial details of the freshwater–saltwater TZ dynamics in response to both sea-level and freshwater-level fluctuations within the physical experiment under transient condition. Such endeavour has also never been attempted in previous experimental studies. The automated image analysis technique implemented here allowed the quantification of the main SWI parameters (toe length and width of TZ) with high spatial and temporal resolution. To further demonstrate the applicability of results and to examine the effect of different aquifer properties on the toe migration and the TZ response to water-level changes, the experiments were carried out twice for two homogeneous systems of different grain sizes. The numerical code SEAWAT was used for validation purposes.

2 | MATERIALS AND METHODS

2.1 | Experimental methods

A laboratory flow tank of dimension 0.38 m × 0.15 m × 0.01 m representing a cross section of an unconfined coastal aquifer was used for the experiments. Figure 1 shows a schematic diagram of the flow tank. The flow tank was subdivided into three distinct compartments: a central chamber and two circular reservoirs located at either side. The central chamber was filled with clear glass beads from Whitehouse Scientific® to simulate the porous medium. Two fine mesh acrylic screens with aperture diameter of 0.5 mm were located at each side of the central chamber to separate the porous medium from the side reservoirs. The apertures of these meshes were small enough to contain the glass beads and sufficiently large to allow circulation of water flowing from the side reservoirs.

The two reservoirs were used to provide constant-head boundary condition at either side of the porous media. The left and right side reservoirs were filled with freshwater and saltwater, respectively. The freshwater reservoir was filled with cold tap water. Adjustable overflow outlets were placed within each reservoir to maintain the water levels by draining any excess water to waste. Each of the overflow outlets was connected to a flexible hose that was plugged at the bottom of each reservoir as shown in Figure 1. The saltwater filling the right side reservoir was sourced from a 200-L saline water solution prepared prior the experiments. The saltwater solution was prepared by dissolving food grade into freshwater at a concentration of 36.16 g/L to achieve a density of 1,025 kg/m^3.

The density of the saltwater solution was monitored using a hydrometer H-B Durac plain-form polycarbonate and through manual measurements using mass/volume ratio. In order to distinguish it from the freshwater, red food colour was added to the saltwater at concentration of 0.15 g/L. The scale used for the measurement of salt and dye quantities was accurate to 0.01 g. For each set of experiments, the saltwater was primarily sourced from the initial 200-L batch in order to reduce any possible risks of density or colour discrepancies between each experiment to a minimum. The water levels in both freshwater and saltwater reservoirs were monitored using ultrasonic sensors Microsonic mic+25/DIU/TC with ±0.2-mm accuracy.

Two homogeneous aquifer systems were simulated in this study, using glass beads of sizes 1,090 and 1,325 μm. The hydraulic conductivity of each of these was estimated using in situ measurement within the experimental flow tank. Various hydraulic gradients were successively imposed to the system, and the corresponding volumetric freshwater discharge was measured. The average hydraulic conductivity value was then subsequently derived using Darcy's law, as described in Oostrom, Hayworth, Dane, and Güven (1992). The average hydraulic conductivity value of the flow tank was estimated at 85 and 108 cm/min, for the beads 1,090 and 1,325 μm, respectively. The porosity of porous media was measured using volumetric method, and an average value of 0.38 was considered for all the beads.

The study included a total of 30 experiments, as shown in Table 1. All the experiments were performed for the two bead sizes 1,090 and 1,325 μm. For each bead size, 10 experiments were completed for the

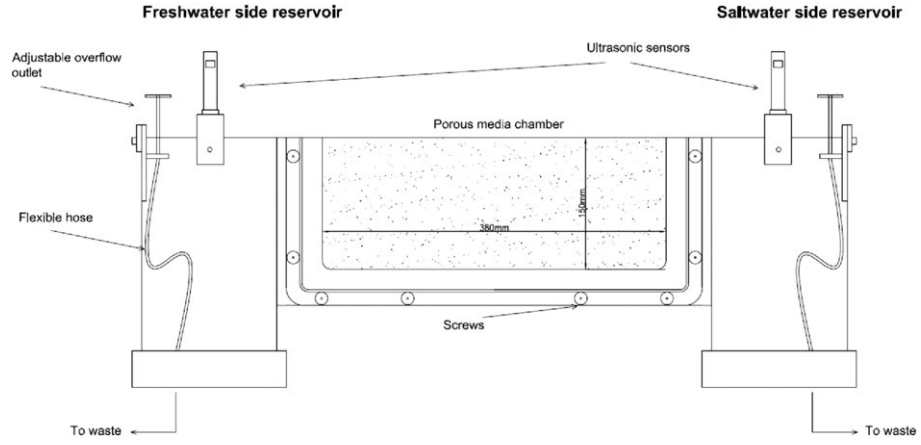

FIGURE 1 Schematic diagram of the porous media tank

TABLE 1 Experimental case investigated in the study, where dh and ΔH refer to the head boundary difference and the head change magnitude, respectively

Experiment	Advancing wedge (FW/SL)	Receding wedge (FW/SL)	Magnitude of inland head change (FW)
1,090	dh = 6, 5.2, 4.4, 3.6 mm	dh = 6, 3.6, 4.4, 5.2, 6 mm	ΔH = 0.8, 1.6, 2.4 mm
1,325	dh = 6, 5.2, 4.4, 3.6 mm	dh = 6, 3.6, 4.4, 5.2, 6 mm	ΔH = 0.8, 1.6, 2.4 mm

Note. In total, 30 experimental cases were carried out.

advancing wedge experiment and receding wedge experiment as a result of gradual freshwater head drop and rise, respectively, whereas the saltwater boundary remained constant. Five additional experiments were completed where the magnitude of the freshwater-level change was varied. Another set of 10 experiments were carried out for the advancing wedge and receding wedge experiments where the saltwater level was changed whereas the freshwater boundary was held constant. The five head differences applied to the system in the advancing wedge experiment were dh = 6, 5.2, 4.4, and 3.6 mm, and the head difference was then returned to the initial value (dh = 6 mm). In the receding wedge experiment, the head difference were applied in reverse order, that is, dh = 3.6, 4.4, and 5.2 mm and back to dh = 6 mm. The set of experiments involving freshwater head variations with constant saltwater boundary is referred to as FW in the forthcoming figures. The sets of experiments where the saltwater level was changed whereas the freshwater boundary was held constant are referred to as SL. The head differences applied in the experiments involving variations in the magnitude of head change were similar to the others: The different head change magnitudes used therein included: 0.8 mm (dh = 6 to 5.2 mm), 1.6 mm (dh = 6 to 4.4 mm), and 2.4 mm (dh = 6 to 3.6 mm).

2.2 | Experimental procedure

A photograph of the whole experimental set-up used in this study is shown in Figure 2. The glass beads were packed into the central chamber under saturated conditions to avoid air bubbles development. The beads were packed in successive even-sized layers, and each layer was carefully compacted to ensure homogeneity of the packing. Two LED lights (Camtree 600) were placed behind the experimental set-up to illuminate the porous media, and a diffuser was fixed to the back of the tank to ensure homogeneity of the light throughout the aquifer. A high-speed camera IDT MotionPro X-Series was used to capture images of the experiments every 30 s for all the experiments. Each time the camera was triggered, 10 images were recorded. The average of these images was then used in the analysis procedure.

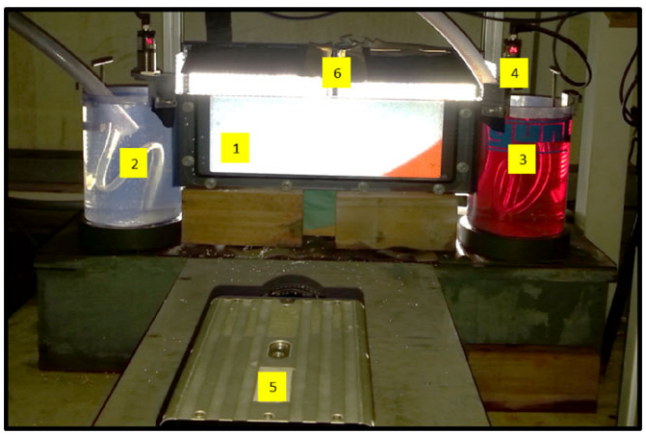

FIGURE 2 Photograph of the experimental set-up: 1 = porous media chamber; 2 = freshwater reservoir; 3 = saltwater reservoir; 4 = ultrasonic sensors; 5 = high-speed camera; 6 = LED lights

To allow the determination the key SWI parameters, each experimental configuration was preceded by a calibration procedure allowing correlation of the saltwater concentration to the intensity of the light transmitting through the main chamber. This calibration is described in thorough details in Robinson et al. (2015). The purpose of the calibration was basically to correlate the saltwater concentration to the intensity of the light transmitting through the main chamber. The calibration procedure consisted in flushing the entire system with various saltwater solutions at known concentrations and recording the image of each saturated aquifer. For every concentration, the light intensity of every single pixel of the system was recorded. The known concentrations and corresponding light intensities were used to derive, through regression analysis, the coefficients a, b, and c of a power law curve expressed by $C = aI^b - c$, adopted to relate the light intensity I and the concentration. The regression analysis was performed through a MATLAB code developed specifically for this purpose (Robinson et al., 2015).

The images recorded over the course of the experiments could thereafter be analysed through another MATLAB code that applied the derived regression coefficients determined in the calibration and analysed each single image to calculate the main intrusion parameters (i.e., toe length and width of TZ) and provided postprocessed images displaying the distribution of salt concentration throughout the system for clear visualization. The toe length was taken as the distance between the 50% concentration isoline and the saltwater boundary along the bottom boundary, and the width of the TZ was measured as the average of the vertical distance between the 25% and 75% saltwater isolines within the range 20% and 80% of the toe length.

Prior to the experiments, freshwater was injected at constant rate from a large tank located above the left side reservoir. The freshwater level was set high enough to allow the entire porous media to remain fully saturated with freshwater. Freshwater flux transited through the system from the inland boundary and exited at the coastal boundary without overflowing. The freshwater exiting the system was rapidly drained out through the overflow outlet of the saltwater reservoir. The later was adjusted such that to maintain a constant saltwater head of 129.7 mm. Excess amount of saltwater was supplied from another large tank into the right reservoir to ensure the prompt flushing out of any freshwater floating at the surface. The density in the saltwater reservoir was continuously monitored using a hydrometer.

The saltwater intrusion experiments were initiated only after stabilization of the density measurements.

The experiments were initiated by lowering the overflow outlet of the freshwater reservoir such that to impose an initial constant freshwater head of 135.7 mm. This initial head boundary difference dh = 6 mm allowed the dense saline water to penetrate into the porous media until the system reached steady-state condition. Steady-state condition was assumed when no substantial changes could be visually observed in the freshwater–saltwater interface position. Various hydraulic gradients were thereafter applied to the system to simulate changes in the hydrological conditions. This was done by varying the freshwater level such that to impose various head differences ranging from dh = 6 mm to dh = 3.6 mm, corresponding to hydraulic gradients of 0.0158 and 0.0095, respectively. These values were within the range of hydraulic gradients values commonly used in previous similar laboratory studies (Chang & Clement, 2012; Goswami & Clement, 2007) as well as within the range of values measured in some real coastal aquifers (Attanayake & Sholley, 2007; Ferguson & Gleeson, 2012).

2.3 | Description of the numerical model

The MODFLOW family variable-density flow code SEAWAT (Guo & Langevin, 2002) was used to perform the numerical modelling experiments. SEAWAT combines the modified MODFLOW (Harbaugh, Banta, Hill, & McDonald, 2000) and MT3DMS (Zheng & Wang, 1999) into a single program that solves the coupled groundwater flow and solute transport equations. SEAWAT has been widely used to solve various variable-density groundwater flow, such as the two box problems, the Henry problem, the Elder problem, and the HYDROCOIN problem (Guo & Langevin, 2002; Langevin, Shoemaker, & Guo, 2003). SEAWAT has also been successfully used for modelling SWI experiments involving freshwater head boundary variations (Chang & Clement, 2012; Goswami & Clement, 2007). The purpose of performing numerical simulations was primarily to assess the consistency of the experimental data with the numerical predictions.

The dimensions of simulation area corresponded to the dimensions of the porous media chamber of the flow tank. The model domain was evenly discretized with a grid size of 0.2 cm. A no-flow boundary condition was set at the top and bottom of the model domain. The longitudinal dispersivity was estimated after trial and error process and was eventually estimated at 0.1 cm, and the transverse dispersivity was 0.05 cm, which is within the range of dispersivity values reported in Abarca and Clement (2009). The spatial discretization satisfies the criterion of numerical stability; that is, grid Peclet number was less than or equal to four (Voss & Souza, 1987). The porosity was set to 0.38. The molecular diffusion was neglected in all the numerical simulations (Riva, Guadagnini, & Dell'Oca, 2015). The specific storage was set at 10^{-6} cm^{-1}. The freshwater density was set to 1,000 kg/m^3, and the saltwater density was set to 1025 kg/m^3. Considering the standard density-concentration slope factor of 0.7, a concentration of 36.16 g/L was used for the seawater boundary.

3 | RESULTS AND DISCUSSION

3.1 | External SWI metrics

The experimental images of the steady-state saltwater wedge for the two cases are shown in Figure 3. In the first experiment, the head difference was varied as a function of the freshwater head boundary, whereas the head at the seaside boundary remained fixed at 129.7 mm. As stated earlier, the first steady-state saltwater wedge after the freshwater boundary head was dropped to 135.7 mm (dh = 6 mm) was considered as the initial condition of the experiment (t = 0.0 min). The saltwater intrusion lengths TL were 7.9 and 8.4 cm in cases 1,090 and 1,325, respectively. The freshwater level was thereafter successively decreased down to 134.9, 134.1, and 133.3 mm, that is, using a constant decreasing step of 0.8 mm. This drastically reduced the freshwater flow through the system, which allowed the saline water to penetrate further inland. The recorded saltwater wedge toe lengths TL were 11.3, 16.5, and 24.9 cm in case 1,090 and 11.5, 17.2, and 25.5 cm in case 1,325, for dh = 5.2 mm (t = 50 min), 4.4 mm (t = 100 min), and 3.6 mm (t = 150 min), respectively. The freshwater level was then increased back to the initial value of 135.7 mm (dh = 6 mm), thereby forcing the saltwater wedge to recede towards the coastline boundary, until the system reached the final steady state.

The steady state of the first stress period (dh = 6 mm) was also considered as the initial condition in the SLR experiments. The inland freshwater level was maintained constant at 135.7 mm, and the saltwater level was successively raised up to 130.5, 131.3, and 132.1 mm to maintain the same head difference decrement pattern as in the freshwater change scenario. This rise of the saltwater level induced an increase of the supply of saline water into the aquifer. The buoyancy forces that drive the intrusion were subsequently increased, thereby enforcing the saltwater wedge to intrude up 11.4, 17.6, and 26.7 cm in case 1,090 and 11.8, 18.3, and 28.2 cm in case 1,325, following the application of dh = 5.2, 4.4, and 3.6 mm, respectively. Likewise, the saltwater wedge was then forced to retreat towards the coastline after the sea level was instantaneously dropped down to the initial value of 129.7 mm.

The numerical model SEAWAT was used for the numerical simulations of the experimental case 1,090 in the FW scenario. The initial condition of the model represented an aquifer with fully freshwater. The transient progression of the saltwater wedge was reproduced over five stress periods. The first stress period was essentially used to set the initial conditions, where the saline water was allowed to enter the model domain and reach a first steady-state condition following the application of a head of 135.7 and 129.7 mm, at the freshwater (C = 0 g/L) and saltwater boundary (C = 36.16 g/L), respectively, like in the experiments.

In the three following stress periods, the freshwater head was successively decreased to establish dh = 5.2, 4.4, and 3.6 mm in each of the three stress periods, respectively. In the last stress period, the freshwater was reset to the initial value (dh = 6 mm), which forced the retreat of the saltwater wedge towards the boundary. Figure 4 presents the comparison between the numerical simulation results and the experimental toe length data. In overall, the results show that

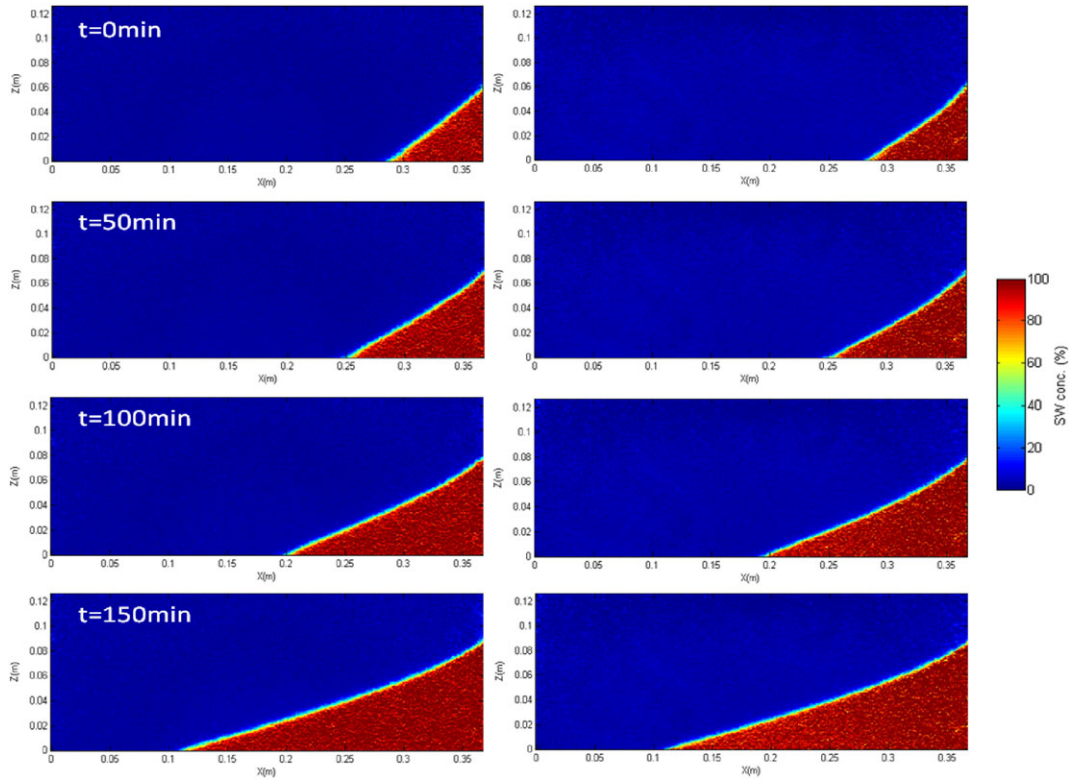

FIGURE 3 Experimental images of the saltwater wedge in case 1,090 (left) and case 1,325 (right)

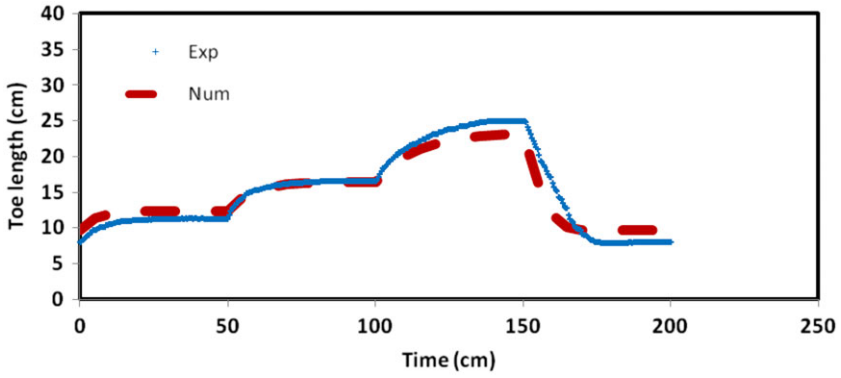

FIGURE 4 Comparison between transient experimental and numerical toe length data

the transient toe movement was reasonably well predicted by the numerical model. The maximum percentage difference was 10%, 1%, and 7% for dh = 5.2, 4.4, and 3.6 mm, respectively. Some mismatch could be observed in the retreat, where the toe movement predicted by the numerical was slightly faster than in the physical model, as observed in previous similar studies (Chang & Clement, 2012; Robinson et al., 2015; Robinson et al., 2016), with a maximum percentage difference recorded at the end of the retreat (nearly 21%).

The transient toe length data for the two cases are shown in Figure 5. As expected, the saltwater intrusion process caused by sea-level changes induced faster and larger intrusion length than that caused by freshwater fluctuations, for the same absolute head change magnitude. Unlike confined aquifers, SLR in unconfined aquifers is associated with an increase of the transmissivity (average saturated thickness) of the system. Although the transmissivity continuously increases with incremental increase of the coastal head boundary, it decreases when dropping the inland head boundary, for equivalent absolute head change. The increase of transmissivity has been found to induce larger inland intrusion length in unconfined aquifers in Chang et al. (2011), which comforts the current observations.

The intruding and receding rates of the wedge were quantified and compared in order to assess the difference in timescale of intrusion and retreat resulting from inland and coastal head changes. The parameter ΔTL was employed to characterize the relative distance to be travelled by the toe before reaching its steady-state value, such that ΔTLi (*t*) = abs [TL(*t*) − TLf]/TLf and ΔTLr (*t*) = abs [TL(*t*) − TLf]/TL0 for the intruding and receding cases, respectively, where TL (*t*) is the toe length at time *t*, TLf is the final steady-state toe length, and TL0 is the toe length prior to the application of the head change. The time to reach steady state corresponds to the time at which ΔTL becomes smaller than 1%. The curves of ΔTL of the intruding and receding wedge phases for the various water-level changes are shown in Figure 6 and the times required for the saltwater toe to reach steady state are presented in Table 2.

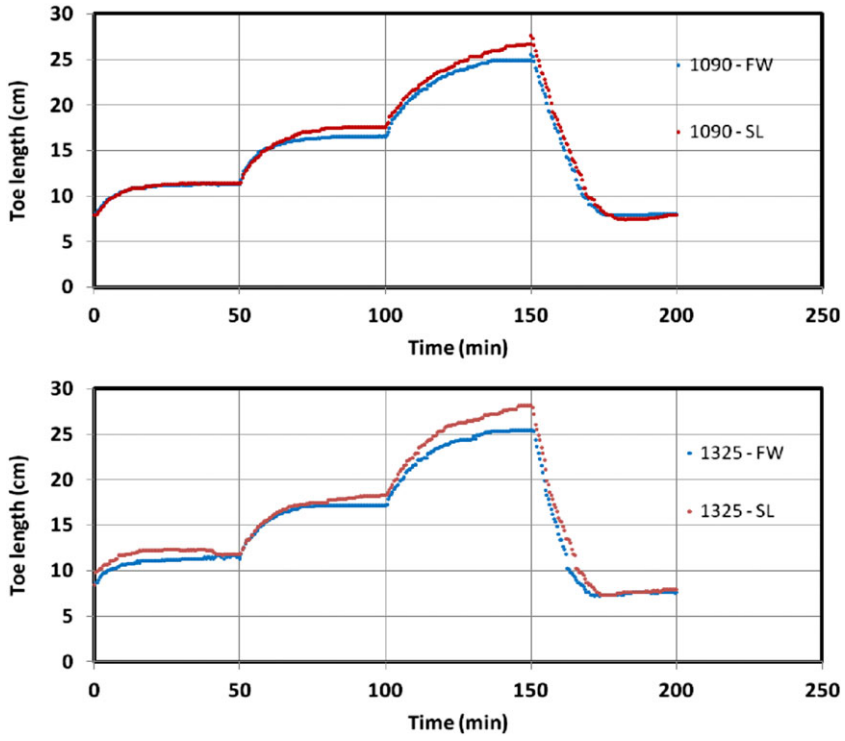

FIGURE 5 Transient experimental toe length data in advancing scenario in case 1,090 (top) and case 1,325 (bottom) for both freshwater (FW) and sea-level (SL) change experiments

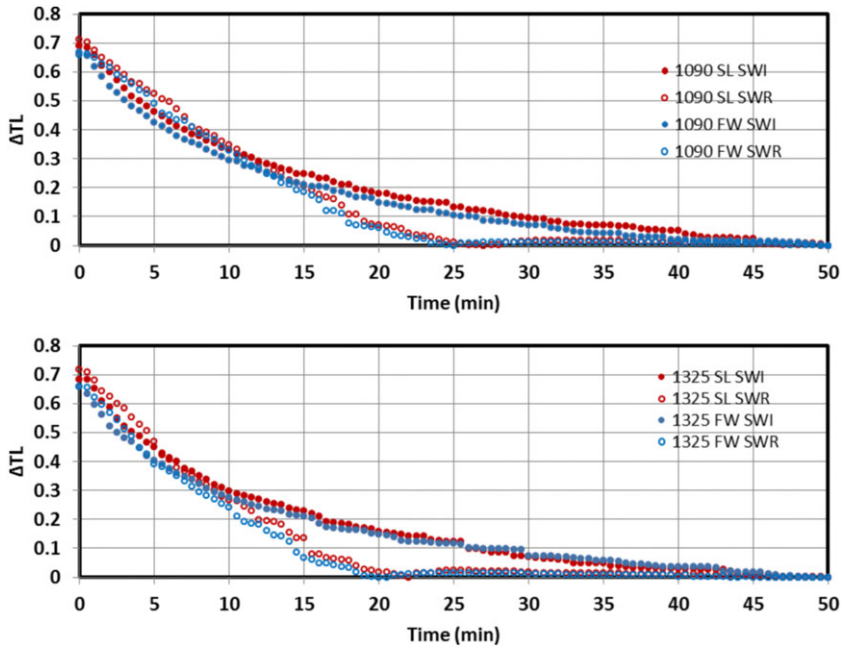

FIGURE 6 Comparison of the toe intruding (seawater intrusion [SWI]) and receding (seawater retreat [SWR]) rates following both freshwater (FW) and sea-level (SL) changes between dh = 6 mm and dh = 3.6 mm (ΔH = 2.4 mm) in case 1,090 (top) and case 1,325 (bottom)

TABLE 2 Time required for the wedge to reach steady-state condition for both freshwater (FW) and sea-level (SL) changes between dh = 6 mm and dh = 3.6 mm (ΔH = 2.4 mm)

Case	SL-SWI (min)	FW-SWI (min)	SL-SWR (min)	FW-SWR (min)
1,090	45.5	47.5	25.5	23.5
1,325	44.5	46	21	19

Note. SWI: seawater intrusion; SWR: seawater retreat.

The intruding wedge was here prompted by decreasing the head difference decrement from dh = 6 mm to dh = 3.6 mm for both freshwater (FW) and sea-level (SL) changes, designated as FW-SWI and SL-SWI in the figure, respectively, whereas the retreat was prompted by reincreasing the head difference from dh = 3.6 mm back to dh = 6 mm, designated as FW-SWR and SL-SWR. The data show that the intruding and receding rates of the wedge as well as the time taken to reach steady state are fairly comparable in SL and FW scenarios. Based on a numerical conceptual model study, Lu and Werner (2013) demonstrated than in confined aquifer systems, inland head change would promote similar transient toe motion and timescale of toe response as coastal head changes, in cases of comparable head variations, but opposite direction. These results provide thus experimental evidence of the applicability of their findings to unconfined coastal aquifer systems.

The data in Figure 6 show that the receding rate of the saltwater wedge was relatively faster than the intruding rate in both SL and FW scenarios, with an intruding wedge requiring up to twice longer time than the receding wedge to reach steady-state condition in case 1,325. Although previous studies demonstrated the asymmetry of timescale between intruding and receding processes following inland head variations (Chang & Clement, 2012; Robinson et al., 2015), the present results suggest that timescale asymmetry would also apply in scenarios involving sea-level fluctuations. Figure 6 also shows that the receding migration rate was relatively faster in case 1,325 than in case 1,090 in both SL and FW scenarios, whereas the intruding rates remain relatively comparable. This can readily be observed in the steepness of the slope at t = 0 min in case 1,325, as well as the shorter time taken to reach steady-state condition in both SL and FW fluctuation scenarios in Table 2. This means that for equivalent magnitude of freshwater-level rise/saltwater-level drop, faster seaward motion of the saltwater wedge would occur in higher hydraulic conductivity media, which is extension of the results of Robinson et al. (2016) to sea-level change scenarios. This trend was also confirmed in Figure 7 and Table 3, where the ΔTL results recorded for two different inland head change magnitudes but similar head difference are presented.

3.2 | Freshwater–saltwater TZ

The comparison between the transient experimental and numerical results is presented in Figure 8. The simulation procedure involved here two additional transient stress periods after establishing the initial condition, where the head differences dh = 3.6 mm and dh = 6 mm were successively imposed in the first and second stress periods, respectively, which was achieved by dropping the freshwater head down to 133.3 mm (t = 0–50 min) and thereafter increasing it back to 135.7 mm (t = 50–100 min), respectively. The results show that the shape of the saltwater wedge was relatively well depicted in the numerical model, although the width of the TZ appears slightly thicker in the numerical model compared with the experimental observations. The width of TZ was the same for the two head differences in the experiments, although it slightly increased in the model after the head difference was decreased. The comparison of the transient experimental and numerical toe length data shows nonetheless good agreement for both the advancing and receding wedge conditions, albeit the retreat of the saltwater wedge was slightly faster in the numerical model, as commonly observed in previous studies (e.g., Chang & Clement, 2012; Robinson et al., 2015).

TABLE 3 Time required for the wedge to reach steady-state condition for various head changes magnitude ΔH

Case	ΔH (mm)	Timescale SWI (min)	Timescale SWR (min)
1,090	1.6	33	18.5
	2.4	47.5	23.5
1,325	1.6	35	13.5
	2.4	46	19

Note. SWI: seawater intrusion; SWR: seawater retreat.

Experimental observation showed that under transient condition, the width of TZ was not only narrow but remains constant throughout the entire advancing wedge phase, regardless of the inland head change magnitude applied (Figure 9). These results further show that the widening of TZ width would be little affected by the drop of the freshwater level causing the inland advancement of the saltwater wedge, regardless of the head change magnitude applied. In addition, the width of the TZ was very similar in cases 1,090 and 1,325, fluctuating within the range of 0.3–0.5 cm, which indicates that the change in aquifer hydraulic conductivity induced insignificant effects on TZ over the course of the intrusion phase, regardless of the inland head drop magnitude applied.

Conversely, Figure 9 shows that the width of the TZ exhibited a noticeable widening during the saltwater retreat process, with a magnitude increasing with increasing freshwater-level increment. The peaks of the widening along with their time of occurrence are shown in Table 4. The results not only show that the widening process seems

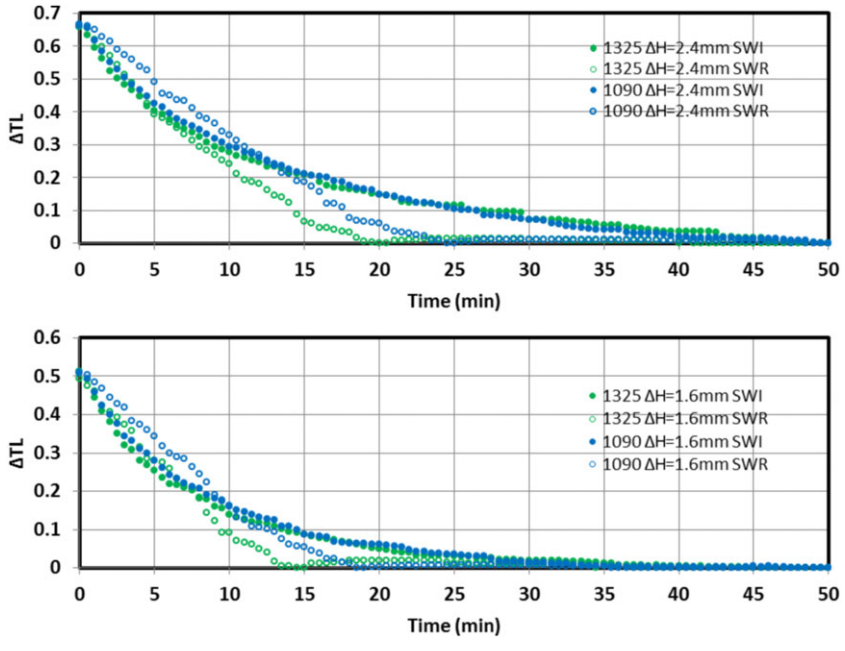

FIGURE 7 Comparison of the toe intruding (seawater intrusion [SWI]) and receding (seawater retreat [SWR]) rates for various inland head change magnitudes. ΔH = 2.4 mm and ΔH = 1.6 mm were simulated by varying dh between dh = 6 mm and dh = 3.6 mm and between dh = 6 mm and dh = 4.4 mm, respectively

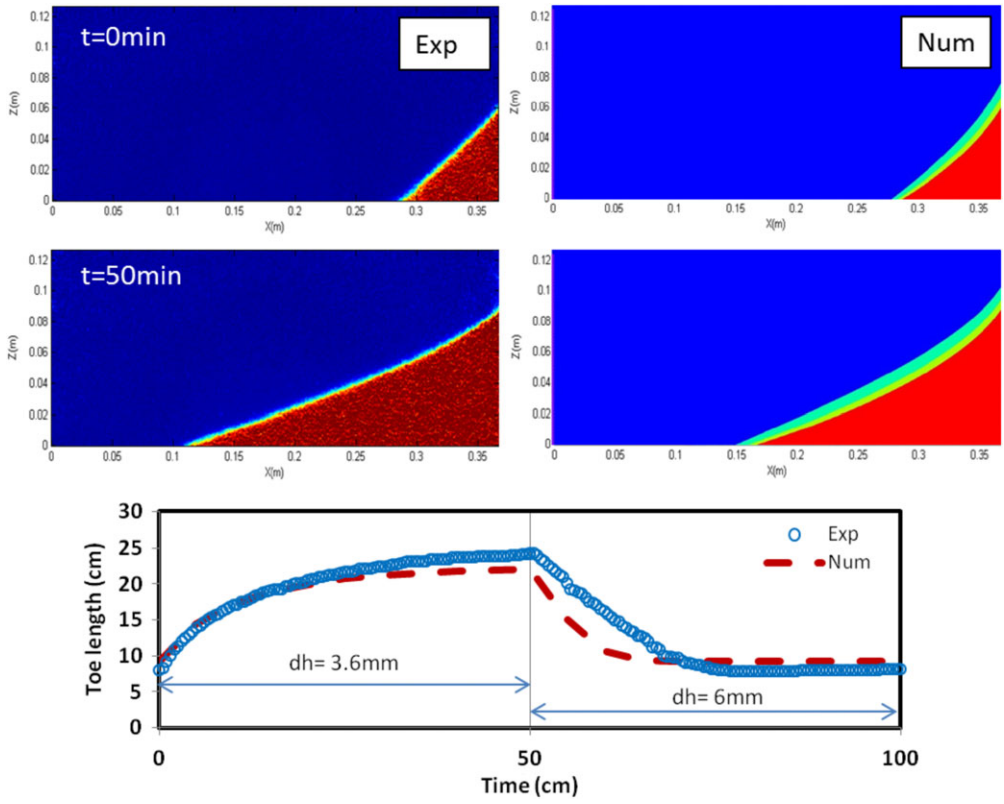

FIGURE 8 Comparison between transient experimental and numerical saltwater wedge for the case 1,090, steady state (top) and transient toe length (bottom). SWI: seawater intrusion; SWR: seawater retreat

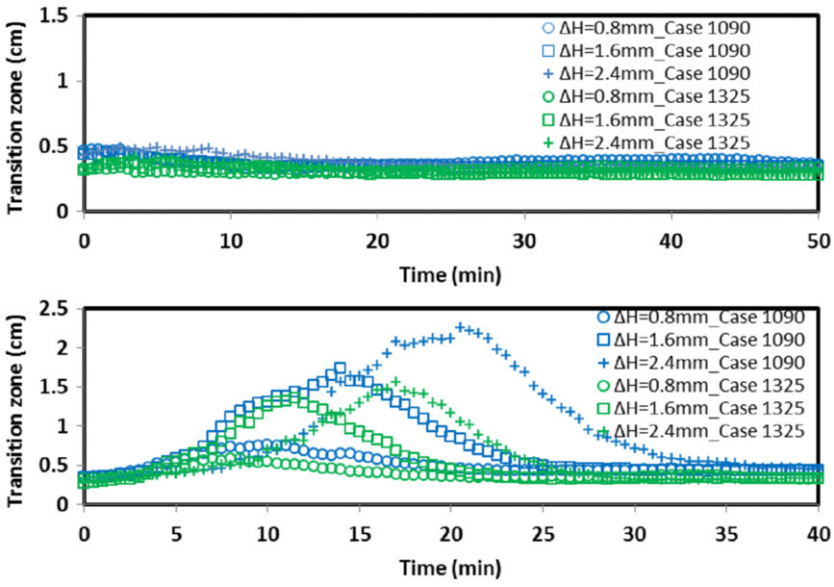

FIGURE 9 Transient transition zone data in the advancing phase (top) and the receding phase (bottom)

TABLE 4 Summary of the maximum values of the transition zone width and their associated time of occurrence

Case	ΔH (mm)	Peak value (cm)	Time to peak (min)
1,090	0.8	0.8	10
	1.6	1.7	14
	2.4	2.3	20.5
1,325	0.8	0.6	7
	1.6	1.4	11.5
	2.4	1.6	17

to be primarily a transient phenomenon but also suggest that the occurrence of the widening may be limited to the seawater retreat process. The magnitude of the head change prompting the seaward motion of the freshwater–saltwater interface is one of the controlling factors of the extent of the widening. The results show that the width of the TZ was nearly 3 times greater from ΔH = 0.8 mm to ΔH = 2.4 mm in both cases 1,090 and 1,325. This is because a higher magnitude of head change would promote higher flow velocity, which implies more dispersion along the interface, thus further increasing the width of the

TZ. The results also show that the TZ occurring during the retreat was also larger when the grain size was smaller (case 1,090). The data show that from the highest (case 1,325) to the lowest grain size (case 1,090), the peak of the widening increased by 33%, 21% and 43%, for ΔH = 0.8, 1.6, and 2.4 mm, respectively.

The response of the width of the TZ to freshwater- and saltwater-level fluctuations during the advancing wedge conditions was analysed, and the results are presented in Figure 10. The results revealed that there was very little change in the width of TZ throughout the SWI process in both scenarios involving freshwater and saltwater head changes. In both cases 1,090 and 1,325, the results show that the width of TZ was fluctuating around 0.3 cm during the entire intrusion process for both head boundary changes. The small variations may solely be due to possible minor fluctuations in the water levels occurring at the boundaries. These observations appear to suggest that the expansion of the TZ would not be significant during the intruding phase of seawater wedge resulting from water table drop or SLR, regardless of the magnitude of the head change.

The transient response of the TZ width exhibited, again, a significant widening of the TZ during the receding wedge phase, with a relatively similar peak magnitude and peak time in both sea-level drop and freshwater rise scenarios (Figure 11). Again, the magnitude of the peak was greater and extended over longer time period in the case of smaller grain size (case 1,090), which further extends the results presented in Figure 9 for scenarios involving sea-level fluctuations. The results therefore give initial indication that the widening of the TZ during the retreat would exhibit the same amplitude in scenarios involving the rise of the water table and a drop of the SLR, in cases of equivalent head change magnitudes but opposite directions.

Figure 12 shows the concentration colour maps of the saltwater wedge during the retreat in both experimental and numerical models. The experimental observations revealed the existence of a yellowish pulse (of relatively low salt concentration) travelling upwards inside the receding saltwater wedge and spreading along the interface, thereby substantially exacerbating the widening of the TZ. This yellowish pulse could be observed about 5 min following the head change and started spreading along the interface at around t = 10 min. The image taken at t = 20.5 min shows the saltwater wedge when the width of TZ reached the maximum peak value. Note that this phenomenon was also observed in the scenario involving saltwater-level fluctuations.

The discrepancies in the toe position between the numerical and physical model results are simply due to the faster receding toe motion observed in the numerical model compared with the physical model, as previously observed in Figure 8. The numerical model reproduced the widening of the TZ width occurring saltwater retreat, although the peak value occurred earlier in the numerical model (within the first 10 min)

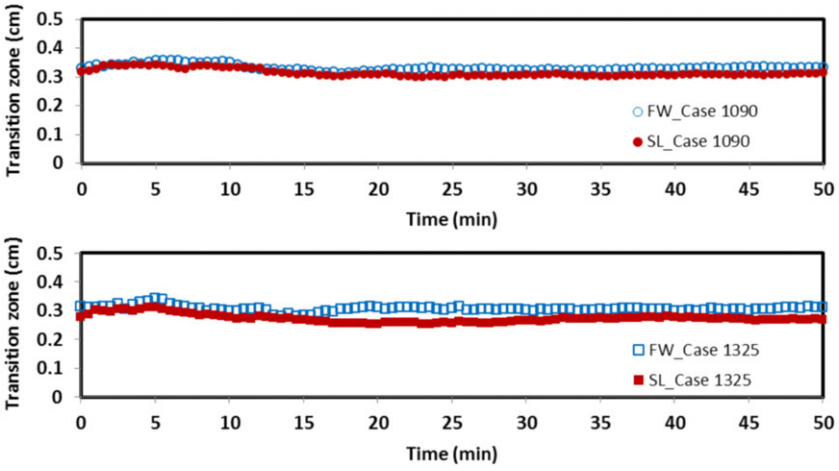

FIGURE 10 Response of the width of the transition zone to decrement of dh from 6 to 3.6 mm (ΔH = 2.4 mm) from both freshwater side (FW) and sea-level side (SL) in case 1,090 (top) and case 1,325 (bottom)

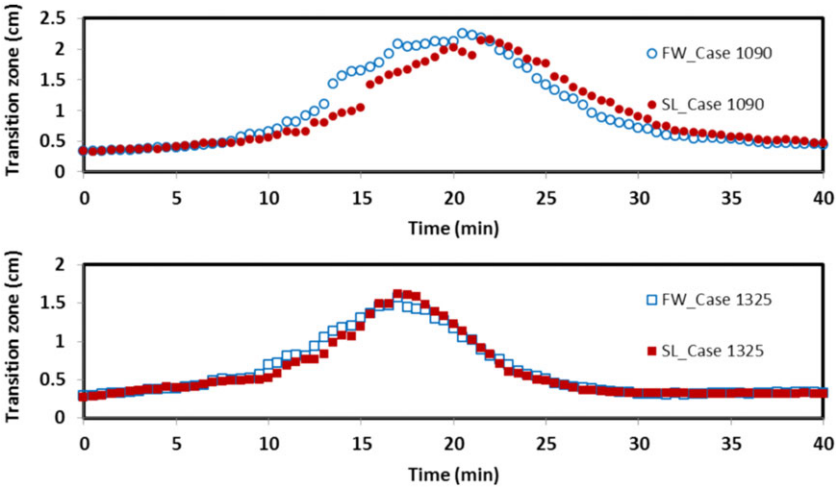

FIGURE 11 Response of the width of the transition zone to increment of dh from 3.6 to 6 mm (ΔH = 2.4 mm) from both freshwater side (FW) and sea-level side (SL) in case 1,090 (top) and case 1,325 (bottom)

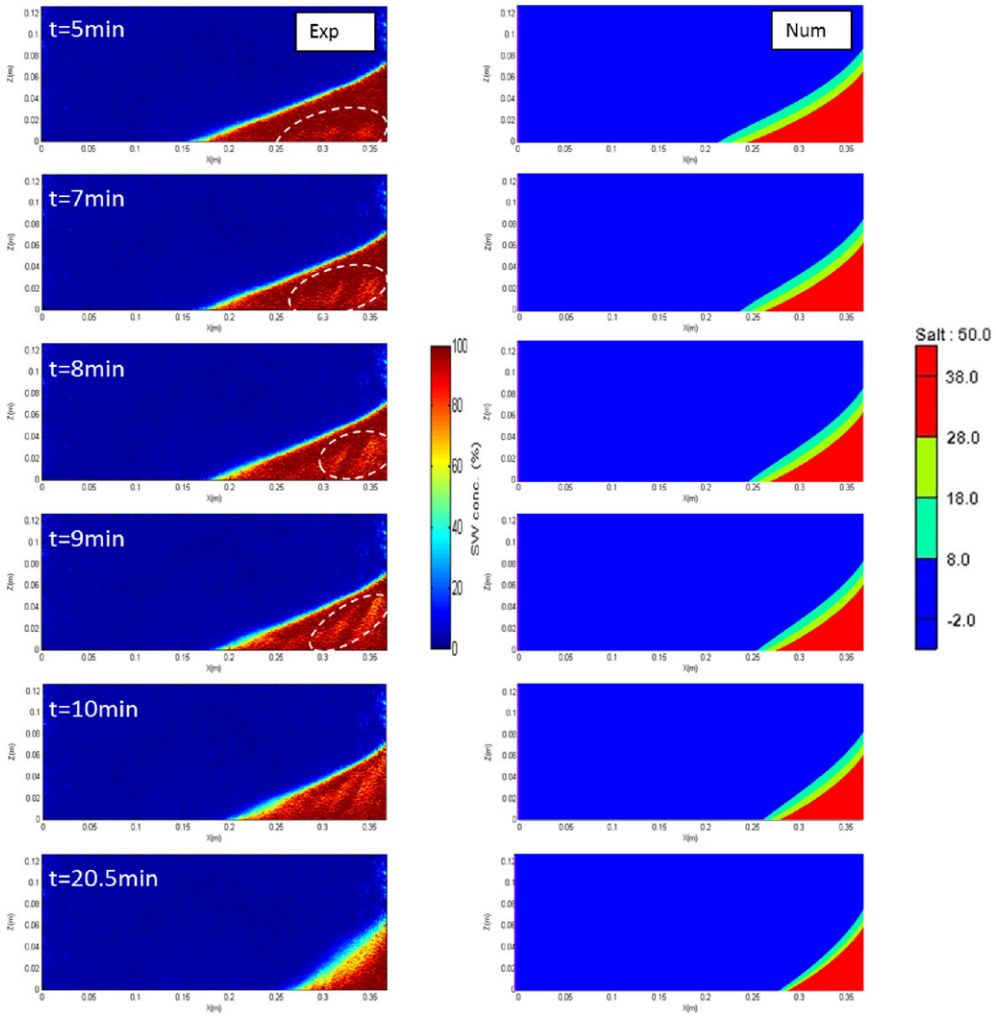

FIGURE 12 Transient experimental and numerical receding saltwater wedge during the receding phase in case 1,090

compared with the physical model (about t = 20.5 min). The widening ended faster in the numerical model compared with the physical experiment, with no noticeable changes observable in the wedge after t = 20 min in the numerical model, whereas changes could still be observed until t = 30 min in the physical experiments. The yellowish pulse could not be reproduced by the numerical simulation, where the widening of the TZ is primarily caused by dispersion along the interface. This further highlights the key role of laboratory experiments in the investigation of density-driven flow in porous media and the evaluation of numerical models (Stoeckl et al., 2015).

It is hypothesized that this yellowish pulse observed in the experiments may have been the results of some freshwater "sliding" into the receding saltwater wedge along the bottom boundary, which was thereafter diluted and sucked upwards towards the interface due to density contrast, thereby exacerbating the widening. This possible sliding freshwater into the wedge may have been caused by the rather sudden rise of the freshwater head that induced in great change of the freshwater flow velocity in the system, thus abruptly pushing seaward the saltwater wedge and creating a perturbation allowing a tiny portion of freshwater to leak along the aquifer bottom. This experimental observation was not an artefact of any wall effects (i.e., 2D vs. 3D transport) given the relatively small width of the tank (10 mm). Despite field evidence of such mechanism have never been documented in previous studies, it is reasonable to hypothesize that such mechanism could conceivably occur in real coastal aquifer systems especially where the non-uniformity aquifer bedrocks may enhance preferential flow. Further investigations would nonetheless be required to examine the reproducibility of this mechanism within larger scale coastal aquifer models, which would enable easier examination of the TZ dynamics.

4 | SUMMARY AND CONCLUSIONS

This study provided a quantitative and qualitative analyses of the effect of boundary water-level variations on saltwater intrusion dynamics and the temporal response of freshwater–saltwater TZ. Two homogeneous cases of different bead sizes (and hence different hydraulic conductivity) were analysed. The main findings of the study are as follows:

- The expansion of the TZ did not occur during the intruding phase of saltwater wedge whether it resulted from freshwater-level drop or saltwater-level rise, regardless of the magnitude of the head change. This finding gives initial indications that in coastal aquifer systems, the widening of the TZ width may not be substantial

during the landward displacement of freshwater–saltwater interface, whether it occurs as a result of water table drop or SLR, regardless of the magnitude of the boundary head change.

- By contrast, a substantial widening of the TZ width was observed during the retreat process, with a peak magnitude and a peak time relatively similar in the scenario involving a rise of the freshwater level relative to the scenario involving a drop of the saltwater level, in cases of equivalent absolute head change magnitudes. This finding suggests that in coastal aquifer systems, receding saltwater wedges induced by a rise of the water table would tend to exhibit TZ expansions of the same magnitude and the same timescale of occurrence as when following a drop of the sea level, provided that the head change magnitudes are comparable but opposite directions.
- The magnitude of the widening of the TZ observed during saltwater retreat was larger and extended over longer time frame in homogeneous aquifers with smaller hydraulic conductivity, irrespectively of whether the head change occurred at the freshwater or saltwater boundary.
- The experimental observations revealed that the widening mechanism was also enhanced by the presence of some freshwater sliding and into the wedge during the saltwater retreat process, which was thereafter sucked upward because of density difference effects and eventually travelled along the TZ towards the outlet, thereby promoting further widening. The observed phenomenon could not be reproduced by the numerical simulation, which underlines the importance of physical model experiments for the investigation of density-driven flow in porous media in improving general process understanding. It seems conceivable that such mechanism could possibly occur in real coastal aquifer systems where the common non-uniformity of aquifer bedrocks could further enhance preferential flow and thus facilitate the leakage of some freshwater below the wedge, albeit field evidence of such effect have never been reported in previous studies. Further investigations involving larger aquifer models would enable further examination of the TZ dynamics and explore the reproducibility of this observed phenomenon at larger scale.
- The transient analysis of the saltwater toe length revealed that in cases of equivalent saltwater-level variations but opposite directions, the intruding wedge required up to twice longer time to reach steady-state condition than the receding wedge. This observation shows that timescale asymmetry between saltwater intrusion and retreat processes would also occur in scenarios involving sea-level fluctuations. When comparing freshwater and saltwater change scenarios, the intruding and receding rates of the saltwater wedge as well as the time taken to reach steady state were fairly comparable.

ACKNOWLEDGMENTS

The authors would like to thank Salissou Moutari for providing valuable comments that helped improve the manuscript. We acknowledge the support of Queen's University Belfast for this research project through a PhD studentship awarded to the first author.

ORCID

Antoifi Abdoulhalik http://orcid.org/0000-0002-0503-7553

REFERENCES

Abarca, E., & Clement, T. P. (2009). A novel approach for characterizing the mixing zone of a saltwater wedge. *Geophysical Research Letters*, *36*(6), L06402. https://doi.org/10.1029/2008GL036995

Abdoulhalik, A., Ahmed, A., & Hamill, G. (2017). A new physical barrier system for seawater intrusion control. *Journal of Hydrology*, *549*, 416–427.

Abdoulhalik, A., & Ahmed, A. A. (2017a). The effectiveness of cutoff walls to control saltwater intrusion in multi-layered coastal aquifers: Experimental and numerical study. *Journal of Environmental Management*, *199*, 62–73.

Abdoulhalik, A., & Ahmed, A. A. (2017b). How does layered heterogeneity affect the ability of subsurface dams to clean up coastal aquifers contaminated with seawater intrusion? *Journal of Hydrology*, *553*, 708–721.

Attanayake, P., & Sholley, M. (2007). Evaluation of the hydraulic gradient at an island for low-level nuclear waste disposal. *IAHS Publication*, *312*, 237–243.

Chang, S. W., & Clement, T. P. (2012). Experimental and numerical investigation of saltwater intrusion dynamics in flux-controlled groundwater systems. *Water Resources Research*, *48*(9), W09527. https://doi.org/10.1029/2012WR012134

Chang, S. W., Clement, T. P., Simpson, M. J., & Lee, K. (2011). Does sea-level rise have an impact on saltwater intrusion? *Advances in Water Resources*, *34*(10), 1283–1291.

Ferguson, G., & Gleeson, T. (2012). Vulnerability of coastal aquifers to groundwater use and climate change. *Nature Climate Change*, *2*, 342–345.

Goswami, R. R., & Clement, T. P. (2007). Laboratory-scale investigation of saltwater intrusion dynamics. *Water Resources Research*, *43*(4), 43, W04418.

Guo, W., & Langevin, C. D. (2002). User's guide to SEAWAT: A computer program for simulation of three-dimensional variable-density groundwater flow.

Harbaugh, A. W., Banta, E. R., Hill, M. C., & McDonald, M. G. (2000). MODFLOW-2000, the U.S. Geological Survey modular ground-water model—User guide to modularization concepts and the ground-water flow process. Open-File Report. U.S. Geological Survey., 134.

Hussain, M. S., & Javadi, A. A. (2016). Assessing impacts of sea level rise on seawater intrusion in a coastal aquifer with sloped shoreline boundary. *Journal of Hydro-Environment Research*, *11*, 29–41.

Ketabchi, H., Mahmoodzadeh, D., Ataie-Ashtiani, B., & Simmons, C. T. (2016). Sea-level rise impacts on seawater intrusion in coastal aquifers: Review and integration. *Journal of Hydrology*, *535*, 235–255.

Ketabchi, H., Mahmoodzadeh, D., Ataie-Ashtiani, B., Werner, A. D., & Simmons, C. T. (2014). Sea-level rise impact on fresh groundwater lens in two-layer small islands. *Hydrological Processes*, *28*, 5938–5953.

Langevin, C. D., Shoemaker, W. B., & Guo, W. (2003). MODFLOW-2000, the US Geological Survey modular ground-water model—Documentation of the SEAWAT-2000 version with the variable-density flow process (VDF) and the integrated MT3DMS transport process (IMT). USGS Open-File Report 03–426. Tallahassee, Florida.

Lu, C., Kitanidis, P. K., & Luo, J. (2009). Effects of kinetic mass transfer and transient flow conditions on widening mixing zones in coastal aquifers. *Water Resources Research*, *45*, W12402.

Lu, C., & Luo, J. (2010). Dynamics of freshwater-seawater mixing zone development in dual-domain formations. *Water Resources Research*, *46*, W11601.

Lu, C., & Werner, A. D. (2013). Timescales of seawater intrusion and retreat. *Advances in Water Resources*, *59*, 39–51.

Michael, H. A., Russoniello, C. J., & Byron, L. A. (2013). Global assessment of vulnerability to sea-level rise in topography-limited and recharge-

limited coastal groundwater systems. *Water Resources Research*, *49*(4), 2228–2240.

Morgan, L. K., Bakker, M., & Werner, A. D. (2015). Occurrence of seawater intrusion overshoot. *Water Resources Research*, *51*(4), 1989–1999.

Morgan, L. K., Stoeckl, L., Werner, A. D., & Post, V. E. A. (2013). An assessment of seawater intrusion overshoot using physical and numerical modeling. *Water Resources Research*, *49*(10), 6522–6526.

Oostrom, M., Hayworth, J. S., Dane, J. H., & Güven, O. (1992). Behavior of dense aqueous phase leachate plumes in homogeneous porous media. *Water Resources Research*, *28*, 2123–2134.

Oude Essink, G. H. P., van Baaren, E. S., & de Louw, P. G. B. (2010). Effects of climate change on coastal groundwater systems: A modeling study in the Netherlands. *Water Resources Research*, *46*, W00F04. https://doi.org/10.1029/2009WR008719

Rasmussen, P., Sonnenborg, T., Goncear, G., & Hinsby, K. (2013). Assessing impacts of climate change, sea level rise, and drainage canals on saltwater intrusion to coastal aquifer. *Hydrology and Earth System Sciences*, *17*(1), 421–443.

Riva, M., Guadagnini, A., & Dell'Oca, A. (2015). Probabilistic assessment of seawater intrusion under multiple sources of uncertainty. *Advances in Water Resources*, *75*, 93–104.

Robinson, G., Ahmed, A. A., & Hamill, G. A. (2016). Experimental saltwater intrusion in coastal aquifers using automated image analysis: Applications to homogeneous aquifers. *Journal of Hydrology*, *538*, 304–313.

Robinson, G., Hamill, G. A., & Ahmed, A. A. (2015). Automated image analysis for experimental investigations of salt water intrusion in coastal aquifers. *Journal of Hydrology*, *530*, 350–360.

Sebben, M. L., Werner, A. D., & Graf, T. (2015). Seawater intrusion in fractured coastal aquifers: A preliminary numerical investigation using a fractured Henry problem. *Advances in Water Resources*, *85*, 93–108.

Sherif, M. M., & Singh, V. P. (1999). Effect of climate change on sea water intrusion in coastal aquifers. *Hydrological Processes*, *13*, 1277–1287.

Stoeckl, L., & Houben, G. (2012). Flow dynamics and age stratification of freshwater lenses: Experiments and modeling. *Journal of Hydrology*, *458–459*, 9–15.

Stoeckl, L., Houben, G. J., & Dose, E. J. (2015). Experiments and modeling of flow processes in freshwater lenses in layered island aquifers: Analysis of age stratification, travel times and interface propagation. *Journal of Hydrology*, *529*, 159–168.

Voss, C. I., & Souza, W. R. (1987). Variable density flow and solute transport simulation of regional aquifers containing a narrow freshwater-saltwater transition zone. *Water Resources Research*, *23*, 1851–1866.

Watson, T. A., Werner, A. D., & Simmons, C. T. (2010). Transience of seawater intrusion in response to sea level rise. *Water Resources Research*, *46*(12), W12533.

Webb, M. D., & Howard, K. W. F. (2011). Modeling the transient response of saline intrusion to rising sea-levels. *Ground Water*, *49*, 560–569.

Werner, A. D., Bakker, M., Post, V. E. A., Vandenbohede, A., Lu, C., Ataie-Ashtiani, B., … Barry, D. A. (2013). Seawater intrusion processes, investigation and management: Recent advances and future challenges. *Advances in Water Resources*, *51*, 3–26.

Werner, A. D., & Simmons, C. T. (2009). Impact of sea-level rise on sea water intrusion in coastal aquifers. *Ground Water*, *47*(2), 197–204.

Zheng, C., & Wang, P. P. (1999). MT3DMS: A modular three-dimensional multispecies transport model for simulation of advection, dispersion, and chemical reactions of contaminants in groundwater systems.

How to cite this article: Abdoulhalik A, Ahmed AA. Transience of seawater intrusion and retreat in response to incremental water-level variations. *Hydrological Processes*. 2018;32:2721–2733. https://doi.org/10.1002/hyp.13214